




Article

Etching Ceramic Samples with Fast Argon Atoms

Alexander S. Metel ^{*}, Sergey N. Grigoriev , Marina A. Volosova, Yuri A. Melnik  and Enver S. Mustafaev 

Department of High-Efficiency Processing Technologies, Moscow State University of Technology STANKIN, Vadkovskiy per. 3A, 127055 Moscow, Russia; s.grigoriev@stankin.ru (S.N.G.); m.volosova@stankin.ru (M.A.V.); yu.melnik@stankin.ru (Y.A.M.); e.mustafaev@stankin.ru (E.S.M.)

* Correspondence: a.metel@stankin.ru; Tel.: +7-903-246-43-22

Abstract: A new approach to stripping surface layers from ceramics with fast atoms is proposed. The existing beam sources do not allow for a stripping rate of more than a few $\mu\text{m}/\text{h}$ to be achieved. Usually, an increase in the etching rate is associated with growing flux density and energy of fast atoms, which can heat the parts of the beam source up to an inadmissible temperature. In the present work, the etching rate was significantly increased at permanent flux density and energy due to an increase in the angle of incidence of fast atoms on the product surface. An increase in the angle of incidence from zero to 80° resulted not only in an increase in the etching rate by several times but also in simultaneous polishing of the surface to a high finishing class.

Keywords: ceramics; surface layer removal; surface roughness; plasma; glow discharge; concentrated beams; angle of incidence; surface sputtering

1. Introduction

The insufficient reliability of parts made from ceramic materials, which manifests itself in a wide range of mean times between failures, is holding back their application in mechanical engineering. This is due to surface defects, which are stress concentrators and lead to accelerated destruction of contact surfaces and complicate the use of advanced ceramic materials.

For this reason, improving the wear resistance of ceramics is an urgent problem that requires new technological solutions. To improve the characteristics of ceramic products, numerous technics are used today, allowing modification of the surface layer. The most popular and economically feasible is applying functional coatings, which improve the performance of metal products. However, applying the same coatings to ceramic products cannot increase their reliability when operating under conditions of increased thermomechanical loads.

Before deposition of the coatings, it is needed, first, to strip the surface layers full of defects. The roughness of chemically stripped substrates can be similar to the roughness of the coated material [1,2]. Long stripping times and toxic waste are the main disadvantages of chemical methods [3]. They can be eliminated using electrochemical dissolution, which is safer for the environment and faster [4].

The cutting edges of currently used tools mainly have wear-resistant coatings [5–7]. Some of them can be used many times after regrinding and recoating. Such recoating is only possible after removal of the worn-out coating [8]. Efficient stripping of the coating should maintain the initial surface of the product.

For stripping the surface layer, a laser is also applied [9]. It is remarkable for minimum damage to the substrate and ecology [10]. However, the sample surface is quite uneven



Academic Editor: Gaetano Granozzi

Received: 14 November 2024

Revised: 18 December 2024

Accepted: 30 December 2024

Published: 6 January 2025

Citation: Metel, A.S.; Grigoriev, S.N.;

Volosova, M.A.; Melnik, Y.A.;

Mustafaev, E.S. Etching Ceramic

Samples with Fast Argon Atoms.

Surfaces **2025**, *8*, 4. <https://doi.org/10.3390/surfaces8010004>

Copyright: © 2025 by the authors.

Licensee MDPI, Basel, Switzerland.

This article is an open access article

distributed under the terms and

conditions of the Creative Commons

Attribution (CC BY) license

(<https://creativecommons.org/licenses/by/4.0/>).

after laser stripping. For this reason, it would be better to act on the samples with broad beams of ions or fast atoms [11–14]. As the sources with heated cathodes are unable to work in reactive gasses, the ion sources with cold hollow cathodes have been produced [15,16].

Since the defective layer thickness formed during the production of a part using the diamond grinding method can reach 4 μm , the removed layer thickness must be $\sim 5 \mu\text{m}$. The etching with fast atoms can include stripping of a surface layer and polishing a rough surface by sputtering the tops of its protrusions.

Another effective means for removing thick surface layers are pulsed electron beams. Accelerated electrons do not sputter materials, but their thermal effect makes it possible to remove surface layers of products. The impact on a surface of a pulse beam with a pulse width of less than 100 μs is determined by the energy density, w , absorbed by the surface during the pulse. For example, processing of the titanium alloy, VT6, at $w \approx 16 \text{ J/cm}^2$ leads to its high-speed heating and subsequent hardening. At $w \approx 18\text{--}20 \text{ J/cm}^2$, a surface layer with a thickness of 2–25 μm melts uniformly and immediately crystallizes with a high cooling rate of up to 10^8 K/s , forming a layer with low roughness, high corrosion resistance, and surface hardness. And only at $w > 50 \text{ J/cm}^2$ a layer with a thickness of several micrometers is removed from the entire surface irradiated by electrons by an explosive mechanism. By removal with pulsed beams layers of a material from a part, it is possible to precisely change its dimensions.

To do this, you can use the Geza-2 accelerator with a 21 cm-diameter multi-point explosive emission cathode with a concave surface area of 350 cm^2 , with its radius of curvature amounting to 60 cm [17]. The accelerator generates a beam with a cross-sectional area of 50–100 cm^2 , electron energy of 50–400 keV, and beam current of 200–500 A, with a pulse width of 5–250 μs . The beam is compressed by a magnetic system.

In [18], the first experiments were carried out on the compression of electron beams obtained using a grid-plasma emitter based on a hollow cathode glow discharge. A 16 cm-diameter concave emission grid was used, with its radius of curvature amounting to 12 cm. At a voltage pulse amplitude between the grid and the accelerating electrode of up to 200 kV, beam current pulses of up to 200 A with a duration of up to 100 μs and higher were obtained. The source of high-voltage pulses was a Marx generator with cutting spark gaps that set the pulse duration.

In the first setup for processing samples with a compressed electron beam, a hollow 30 cm-high voltage insulator with an internal diameter of 30 cm was mounted on a 50 cm-diameter and 40 cm-high vacuum chamber (Figure 1). A hollow anode with a diameter of 28 cm and a length of 45 cm was fixed inside the insulator, and inside it a 26 cm-diameter and 40 cm-long hollow cathode was mounted. At the upper end of the hollow cathode, there was an ignition electrode, through which the working gas was supplied and an auxiliary cathode.

The lower end of the hollow cathode was covered with a diaphragm having a 5 cm-diameter hole in the center, and the lower end of the anode was covered with a concave 26 cm-diameter grid the radius of curvature of its surface amounting to 26 cm. In a 13 cm-diameter hole at the bottom of the chamber, a 20 cm-long cylinder with an internal diameter of 12 cm was installed coaxial with the hollow anode. An accelerating electrode with a 10 cm-diameter central hole was fixed on the cylinder top, which can be moved along the axis of the hollow anode, changing the distance between the accelerating electrode and the grid from 10 to 15 cm.

Outside the chamber, a water-cooled, removable hollow collector with a diameter of 16 cm and a length of 35 cm is connected to the hollow cylinder. It is isolated from the cylinder, which makes it possible to obtain using a Rogowski coil oscillograms of the current pulses of electrons flying into the collector. The collector is limited from below by a

removable flange on which the sample holder is mounted. After the chamber is filled with air, the flange with the holder is disconnected from the collector and samples are installed inside it to study the beam and its effect on materials. As protection against X-ray radiation, a shield made of a 9 mm-thick lead sheet is installed around the collector.

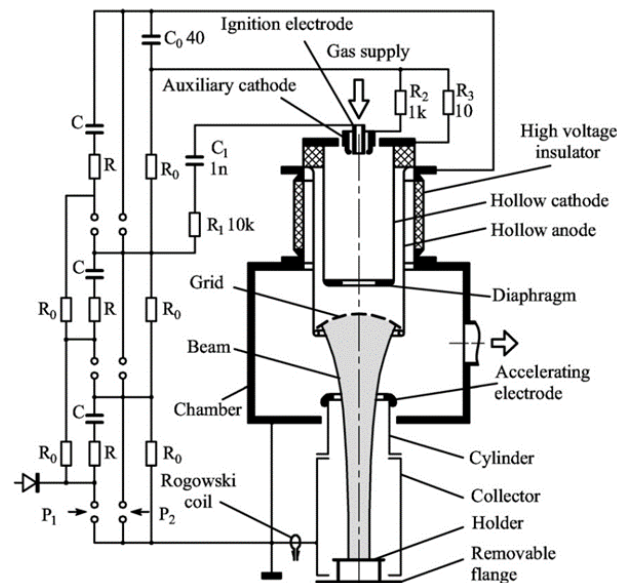


Figure 1. Experimental setup for stripping the surface layer of a sample by electron beam.

The power supply of the setup was a pulse generator according to the Marx circuit of three batteries with a capacity of $C = 0.8 \mu\text{F}$ (2 capacitors IK-100-0.4 in each), charged from a high-voltage rectifier to a voltage of 40–60 kV through resistors $R_0 = 5 \text{ k}\Omega$ and resistors $R = 130 \Omega$. An additional battery with a capacity $C_0 = 40 \mu\text{F}$ was connected in series with the third battery of the generator. When charging all stages to 50 kV, it was charged to a voltage of $\sim 1 \text{ kV}$. Its positive pole was connected to the hollow anode, and the negative pole was connected through $1 \text{ k}\Omega$ and 10Ω resistors to the auxiliary cathode and the hollow cathode, respectively. The ignition electrode installed inside the auxiliary cathode was connected through a resistor with a resistance of $R_1 = 10 \text{ k}\Omega$ and a capacitor with a capacitance of $C_1 = 1 \text{ nF}$ to the spark gaps of the third stage.

When the controlled spark gap of the generator P_1 started, the uncontrolled spark gaps of the second and third stages of the generator were triggered simultaneously with it. As a result, the capacitors of all three stages were connected in series and a pulse with an amplitude of approximately 150 kV was applied to the gap between the grid and the accelerating electrode. The penetration of glow discharge plasma through the hole in the diaphragm of the hollow cathode into the hollow anode was accompanied by the extraction of electrons from it through the holes of the concave grid and their acceleration by a voltage of $U = 150 \text{ kV}$ between the grid and the accelerating electrode.

Measurements of the diameter of the beam imprint on targets made of a 1.0 mm-thick titanium sheet installed in the collector showed that with an increase in the width of the gap between the grid and the accelerating electrode from 10 to 15 cm, the beam diameter near the bottom of the collector practically did not change and was $\sim 6 \text{ cm}$. One of the titanium substrates partially covered with tungsten mask was exposed to five pulsed electron beams, following each other at intervals of 30 s. After removal of the mask, the height of the step between the open and masked surfaces was measured. The step of $22 \mu\text{m}$ for 150 s means the stripping rate of $22 \times 3600/150 = 528 \mu\text{m/h}$. This is an order of magnitude higher than ion sputtering.

The achieved pulsed electron beams have several advantages compared to other means of precision parts processing. They make it possible to reduce the thickness of the removed material layer to almost zero and control the processing by the number of successive pulsed electron beams. The main disadvantage of electron beams is the emission of dangerous personal X-rays.

The sputtering rate defines whether the fast argon atoms are suitable for stripping the surface layer. In industrial practice, pumping out a process vacuum chamber after loading products to be processed takes 15–20 min. Therefore, there is no particular reason to reduce the processing time to less than the pumping time. Anyway, the stripping time should not exceed ~20 min, which is enough to pump out the chamber after placing samples in it. For this reason, to remove a 3 μm -thick surface layer for 20 min, the sputtering rate must be $\sim 3/20 \mu\text{m}/\text{min} = 9 \mu\text{m}/\text{h}$.

Sputtering rate can be increased with the energy of fast atoms and their current. However, it can heat the accelerating grid and other parts of the beam source to an inadmissible temperature. In the present work the etching rate was increased at permanent flux density and energy due to increase in the angle of incidence to the product surface of fast atoms. Growing the angle of incidence from 0 to 80° resulted in an increase in the sputtering rate of the ZrO_2 sample from 4.8 to $11.5 \mu\text{m}/\text{h}$.

2. Materials and Methods

An experimental system for sputtering products is presented in Figure 2. It consists of a rectangular housing and a vacuum chamber. The housing length is 50 cm, width is 20 cm, and height is 15 cm. They are connected through a 130 mm-wide and 80 mm-high rectangular opening in the wall of the chamber. Both vacuum vessels are evacuated through a vacuum channel on the housing bottom by a turbomolecular pump.

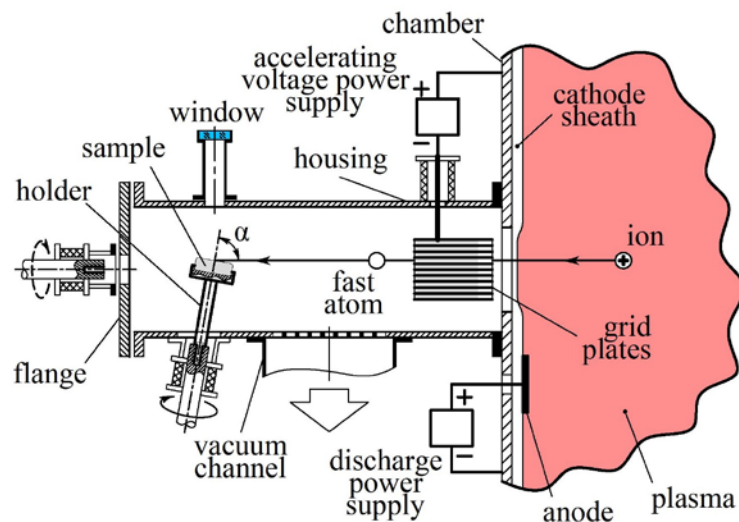


Figure 2. Experimental system for products etching.

An accelerating grid composed of fifteen plates with a thickness of 0.5 mm at 4.5 mm from each other closes the opening. The grid is 70 mm high, 120 mm wide, and 50 mm thick. It is rigidly fastened to the housing with ceramic isolators. Between the chamber and the grid, a source of accelerating voltage is connected.

A rotating sample holder is located inside the housing. The angle between the rotating rod of the sample holder and the axis of the housing is 80° . Consequently, the surface of the sample rotating on the holder is bombarded with fast argon atoms at an angle of incidence

on its surface of $\alpha = 80^\circ$. A quartz window on the housing top makes it possible to observe the sample and measure its temperature with a pyrometer.

A fixed sample holder is mounted in the center of the housing flange facing the accelerating grid. After removing from the housing the rotating holder, it allows the sample to be fixed on the axis of the housing. It only can be moved along the housing axis. Consequently, the surface of the sample is bombarded with fast argon atoms moving perpendicular to its surface. In this case, the sample is pressed against the holder by a titanium strip. The strip is also used as a mask, covering a part of the sample surface facing the grid from fast atoms sputtering it. The gas pressure is regulated with a gas supply arrangement.

Switching on the gas discharge power supply and accelerating voltage power supply initiates the discharge. With the increase in voltage, U , between the chamber and the grid, the grid current, I_g , also increases. When, however, the width of the grid sheath exceeds half the distance between the grid plates, a sharp drop in current, I_g , occurs (Figure 3), and in the housing, the discharge glow expires.

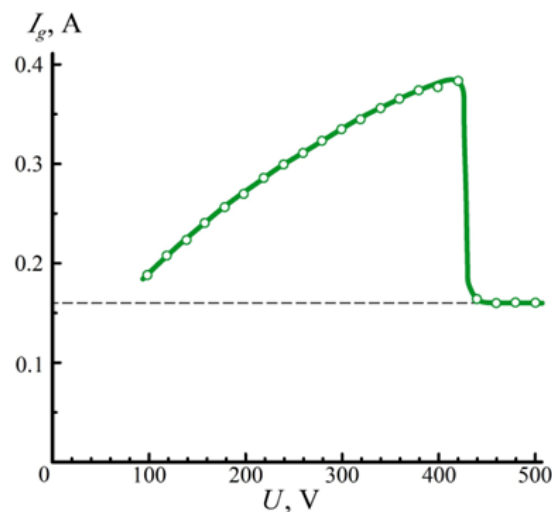


Figure 3. Dependence of the grid current I_g on voltage U at pressure $p = 0.2$ Pa and current $I_d = 2$ A.

The grid prevents electrons from entering the housing and this excludes discharge in it. The grid current, I_g , is the sum of currents of ions from plasma and electrons emitted by the grid. At voltages not exceeding 500 V, the coefficient of secondary emission is less than 0.1 [19,20]. Therefore, the current of secondary electrons can be neglected, and I_g can be assumed as the ion current to the grid. The current, I_g , rises again at $U > 1$ kV.

The chamber and grid surface areas are $S = 0.69$ m² and $S_g = 0.07$ m², respectively. When the discharge current $I_d = 2$ A, the ion current density is equal to $j = I_d / (S + S_g) = 2 / 0.76 = 2.63$ A/m².

When sputtering an iron sample, the maximum sputtering rate is about 2 $\mu\text{m}/\text{h}$. It means that the required rate of the surface stripping of 10 $\mu\text{m}/\text{h}$ cannot be provided by sputtering with the above equipment.

3. Results

For experimental investigations, a number of samples with length and width of 16 mm and thickness of 8 mm have been produced from silicon nitride and zirconium oxide ceramics. Before the treatment, the sample surface was partially covered with a mask, which allowed measurement of the removed surface layer thickness.

To obtain the fast atom distribution across the beam cross-section, a 2 mm-thick titanium target was installed in the housing, located 30 cm from the grid. The target surface

facing the grid was covered with a mask. After sputtering the target, it was unmasked and profilograms of its surface were obtained with a Dektak XT stylus profilometer manufactured by Bruker Nano, Inc. (Billerica, MA, USA). Measurement of the height of a step between the profilogram parts corresponding to the open surface of the target and the surface covered with mask gave the removed layer thickness. Figure 4 shows the distribution of the thickness of the removed layer, Δ , by the height, δ , of the beam cross-section. The thickness, Δ , keeps a constant value of $1.4 \mu\text{m}$ at the distance from the beam axis not exceeding 35 mm and falls to zero outside this interval. It gives evidence of a uniform distribution of the fast atoms.

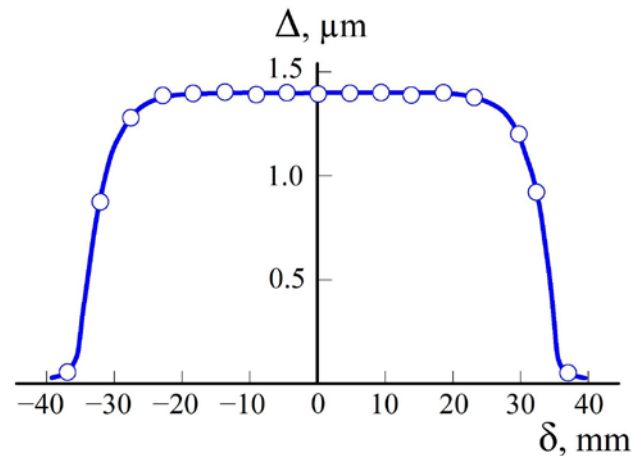


Figure 4. Distribution of removed layer thickness, Δ , on the height, δ , of the beam cross-section.

After a silicon nitride sample with a mask was fastened to the immovable holder, the vacuum chamber was evacuated, and an argon pressure of 0.2 Pa was established. After the power supplies were turned on, a discharge was established. Through the quartz window, it was possible to observe the light of the discharge at current $I_d = 2 \text{ A}$ and accelerating voltage of $U = 6 \text{ kV}$, which penetrated into the housing through the gaps between the grid plates.

The window made it possible to measure the temperature of the sample with an infrared pyrometer. In ten minutes, the sample temperature increased to $500 \text{ }^\circ\text{C}$. After etching the sample for 0.5 h , it was cooled in vacuum and removed from the chamber. The height of the step between the sample surface covered with the mask and its open surface measured with profilometer was equal to $1.1 \mu\text{m}$ (Figure 5). Hence, the sample etching rate amounted to $2.2 \mu\text{m/h}$. When ZrO_2 was investigated, measurements yielded an etching rate of $4.8 \mu\text{m/h}$.

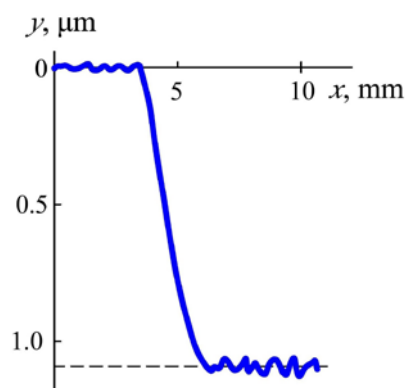


Figure 5. A step between the masked surface (left) and the exposed surface (right) on the profilogram of a silicon nitride sample surface.

After the etching rate of ceramic samples was measured, their surface roughness was investigated. Figure 6 shows profilograms of samples made from two materials: silicon nitride and zirconium oxide before the etching (left) and after the etching (right). The roughness was measured with a profilometer Dektak XT. After etching for half an hour, the roughness decreased from $Ra = 0.116 \mu\text{m}$ to $Ra = 0.105 \mu\text{m}$ for the sample made from silicon nitride and from $Ra = 0.134 \mu\text{m}$ to $Ra = 0.122 \mu\text{m}$ for the sample made from zirconium oxide.

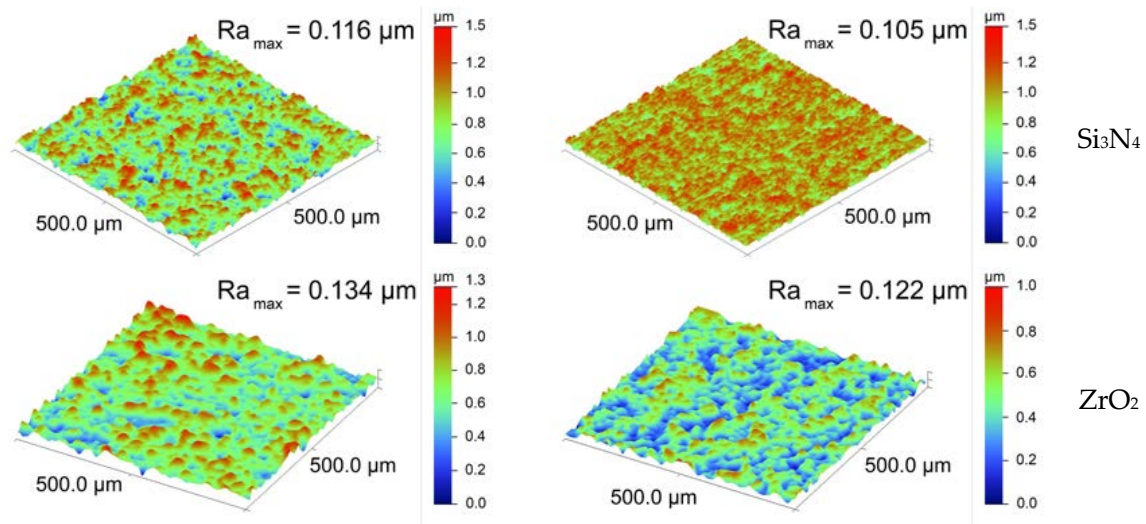


Figure 6. Profilograms of the sample surfaces before (left) and after (right) etching for 0.5 h.

After etching on the immovable holder, ceramic samples with masks on their surfaces were fastened one after another to rotating holder (Figure 2) and subjected to etching for 0.5 h with fast argon atoms at a large angle of incidence of $\alpha = 80^\circ$ on the sample surface. Figure 7 presents dependencies of the removed layer thickness, δ , and surface roughness, Ra , on the summary time of etching a sample made from silicon nitride. Etching for the first half an hour removed a $2.6 \mu\text{m}$ -thick surface layer and decreased the surface roughness from $Ra = 0.105 \mu\text{m}$ to $Ra = 0.031 \mu\text{m}$.

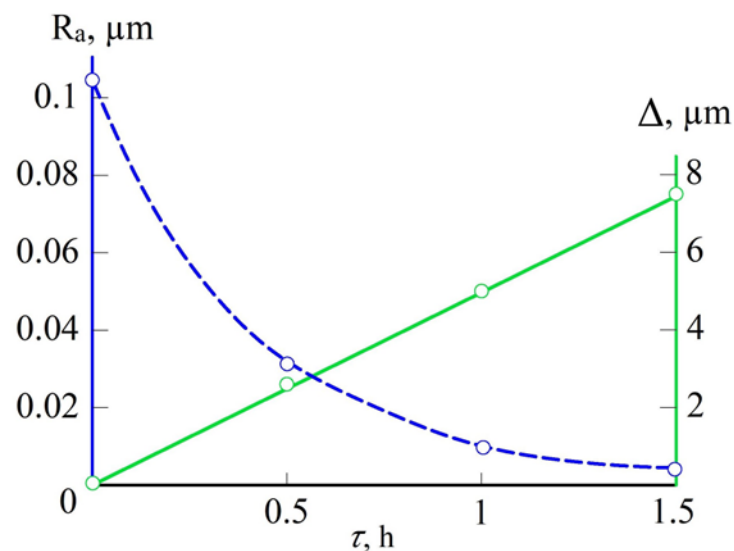


Figure 7. Dependence of the removed layer thickness, Δ , and surface roughness, Ra , of the Si_3N_4 sample on time, τ , of sputtering it at the angle of incidence $\alpha = 80^\circ$.

Then, the sample with a mask was repeatedly fastened to the rotating holder and etched for more half an hour. It resulted in stripping a $2.5 \mu\text{m}$ -thick surface layer and

decrease in the surface roughness from $R_a = 0.031 \mu\text{m}$ to $R_a = 0.0092 \mu\text{m}$. After the third treatment of the sample for half an hour, the thickness of the removed surface layer amounted to $2.4 \mu\text{m}$, and the surface roughness decreased to $R_a = 0.0046 \mu\text{m}$.

The same measurements of the removed layer thickness and surface roughness were carried out for the sample made from zirconium oxide (Figure 8). Etching for the first half an hour removed a $5.4 \mu\text{m}$ -thick surface layer and decreased the surface roughness from $R_a = 0.122 \mu\text{m}$ to $R_a = 0.031 \mu\text{m}$. After the second treatment of the sample for half an hour, a $5.6 \mu\text{m}$ -thick surface layer was removed from the sample, and the roughness of its surface decreased from $R_a = 0.031 \mu\text{m}$ to $R_a = 0.012 \mu\text{m}$. The third treatment resulted in a decrease in the surface roughness from $R_a = 0.012 \mu\text{m}$ to $R_a = 0.0052 \mu\text{m}$ and removal of a $5.5 \mu\text{m}$ -thick surface layer.

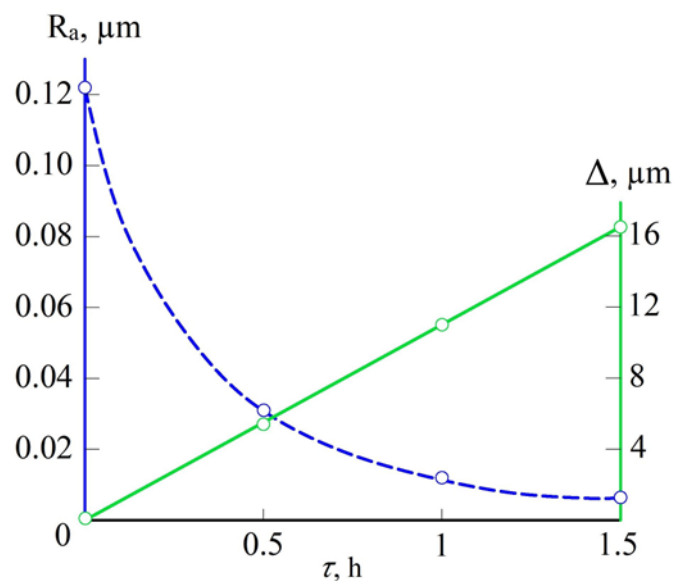


Figure 8. Dependence of the removed layer thickness, Δ , and surface roughness, R_a , of the ZrO_2 sample on time, τ , of sputtering it at $\alpha = 80^\circ$.

The above results show that the etching rate of ceramic samples with fast argon atoms at a large angle of incidence, $\alpha = 80^\circ$, exceeds by several times the etching rate of the samples at a small angle of incidence, $\alpha \sim 0^\circ$. In both cases, at a discharge current $I_d = 2 \text{ A}$ and accelerating voltage of $U = 6 \text{ kV}$, the etching rate of the Si_3N_4 sample keeps a constant value of $\sim 2.2 \mu\text{m}/\text{h}$ at a zero angle of incidence and $\sim 5.2 \mu\text{m}/\text{h}$ at $\alpha = 80^\circ$. In Figure 9 are presented SEM images of samples made from silicon nitride ceramics before etching with fast argon atoms at a large angle of incidence, $\alpha = 80^\circ$ (left image) and after the etching (right image). As for the surface roughness, at zero angle of incidence, it remained practically unchanged, and at $\alpha = 80^\circ$ it decreased by approximately 23 times from $R_a = 0.105 \mu\text{m}$ to $R_a = 0.0046 \mu\text{m}$ after one and a half hours of etching.

At the same discharge current of $I_d = 2 \text{ A}$ and accelerating voltage of $U = 6 \text{ kV}$, measurements yielded the etching rate of $4.8 \mu\text{m}/\text{h}$ for a ZrO_2 sample at zero angles of incidence. The roughness of the sample made from zirconium oxide amounted to $R_a = 0.122 \mu\text{m}$. After the one and a half hour etching, the roughness decreased only negligibly.

As to the etching at the angle of incidence $\alpha = 80^\circ$, the etching rate of the ZrO_2 sample was $11.5 \mu\text{m}/\text{h}$ and exceeded the etching rate for zero angle of incidence by 2.4 times. At the same time, its surface roughness decreased by approximately 24 times from $R_a = 0.122 \mu\text{m}$ to $R_a = 0.0052 \mu\text{m}$ after etching for one and a half hours.

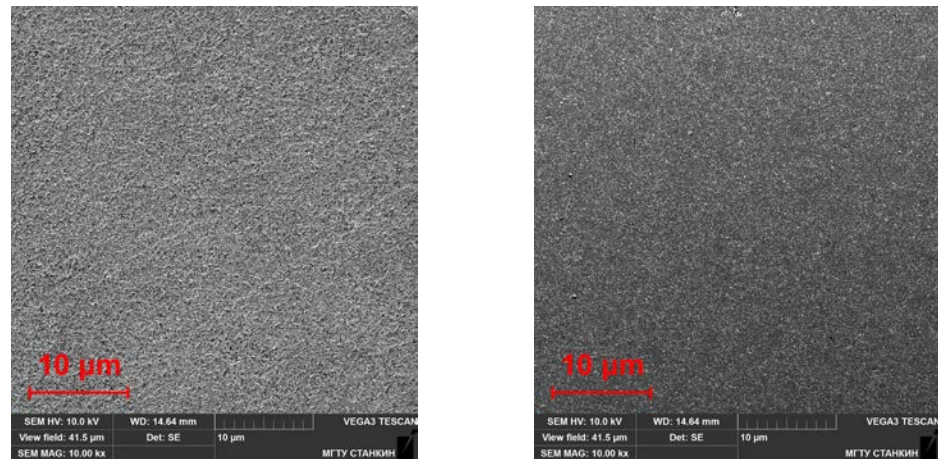


Figure 9. SEM images of Si_3N_4 samples before etching ($R_a = 0.105 \mu\text{m}$, left) and after etching in rotation at an angle of incidence $\alpha = 80^\circ$ ($R_a = 0.0046 \mu\text{m}$, right).

To determine how the sputtering changes the friction of ceramic samples, a precision tribometer Tetra Basalt N2 Falex Tribology NV (Rotselaar, Belgium), was used as a testing machine. Figure 10 presents dependences of the friction coefficient μ on the sputtering time for samples made from Si_3N_4 and ZrO_2 .

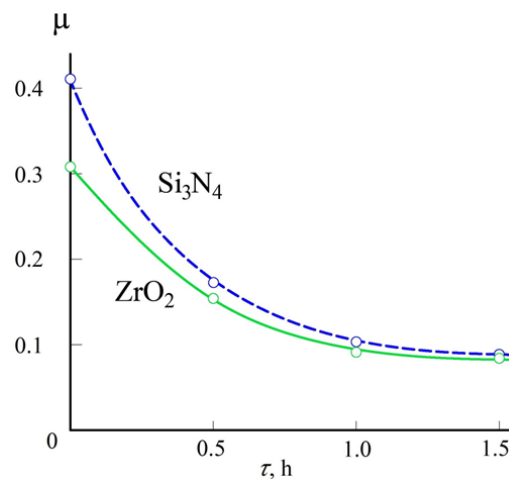


Figure 10. Dependence of the friction coefficient, μ , on the sputtering time, τ , for samples made from silicon nitride (Si_3N_4) and zirconium oxide (ZrO_2).

The initial values of the friction coefficient $\mu = 0.4$ for the Si_3N_4 sample and $\mu = 0.3$ for the ZrO_2 sample after half an hour of etching decreased to $\mu = 0.18$ and $\mu = 0.15$, respectively. The rate of decrease in friction coefficients diminishes with time, τ , and at $\tau = 1.5$ h for both ceramics $\mu \approx 0.1$.

Elemental analysis carried out with a VEGA3 LMH scanning electron microscope (Tescan, Brno, Czech Republic) did not find any changes in the chemical composition of the sample surface after etching it.

Using a Calotest instrument produced by CSM Instruments (Alpnach, Switzerland), it was found that sputtering the ceramic samples with fast argon atoms at the angle of incidence $\alpha = 80^\circ$ improves their abrasion resistance.

A rotating ball was placed on the sample with a load of 0.2 N, and into the contact zone an abrasive suspension was fed. Abrasive particles in the contact zone and applied external force led to local abrasion of the sample surface. The rotating ball produces on the sample surface a spherical wear notch. The notch diameter, D , was measured using an

optical microscope. When D is much smaller than the ball radius, R , the volume of worn material is equal to $V = \pi \cdot D^4 / 64R$.

Figure 11 presents dependencies on the test time of the abrasion volume for zirconium oxide and silicon nitride samples before treatment and after sputtering for one and a half hours the ceramic samples with fast argon atoms at the angle of incidence $\alpha = 80^\circ$. They show that sputtering ceramic samples at a large angle of incidence on the sample surface diminishes the abrasion volume by ~ 1.5 times.

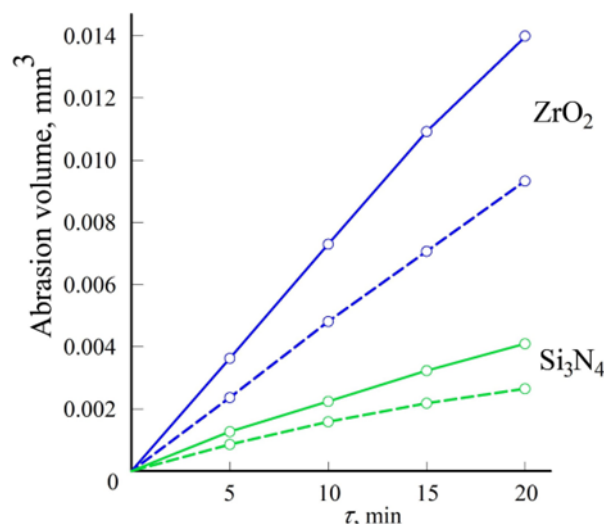


Figure 11. Abrasion volume versus the test time, τ , for ceramic samples before treatment (full lines) and after sputtering for one and a half hour with fast argon atoms at the angle of incidence $\alpha = 80^\circ$ (dashed lines).

The increase in abrasion resistance can be explained by the removal of defective layers from the samples, which leads to compaction of the surface material.

4. Discussion

The obtained results show a new possibility for increasing the rate of stripping of the surface layer from various products. Previously, this problem was solved by increasing the flux density and energy of accelerated particles bombarding the product. When the flux and energy of accelerated particles reach the maximum values achievable with the existing beam source, the flux density can be further increased by compressing the flux [21].

To compress a circular cross-section beam, the flat accelerating grid of the beam source is replaced with a concave grid. Ions accelerated in the sheath between the plasma emitter and the grid pass through the grid holes perpendicular to its surface and turn into fast neutral atoms [22,23]. Their trajectories pass through the grid focal point. With an initial beam diameter equal to the grid diameter of 20 cm, it reaches a minimum value of 1 cm at a distance of 20 cm from the grid. Then, it grows with a further increase in distance. Of course, etching any product in the vicinity of the focal point of the grid allows a removal rate exceeding $10 \mu\text{m}/\text{h}$. However, an increase in the etching rate is associated in this case with growing flux density and energy of fast atoms, which can heat the equipment parts up to inadmissible temperature.

At the same time, fast argon atoms knocking out atoms from the crystal lattice of the product spend about the same energy of ~ 20 eV for each atom. At the initial energy of a fast argon atom of 6000 eV, it should produce about 300 atoms. However, the experimental value of the sputtering coefficient is by two orders of magnitude lower. This is because of the increase in the depth of fast atom penetration into the material with increasing energy, ϵ . Despite the increase in the number of atoms knocked out of the crystal lattice nodes by

the ion, which is proportional to the energy, ϵ , the number of atoms capable of reaching the product surface decreases because of the increase in the length of their path to the surface [24].

When we bombard the surface at a large angle of incidence $\alpha = 80^\circ$, the penetration depth of fast atoms diminishes, the length of the path to the product surface of knocked down atoms decreases, and the sputtering coefficient increases. In our case, at the energy of fast argon atoms of 6000 eV, it resulted in an increase in the sputtering rate from 4.8 $\mu\text{m}/\text{h}$ to 11.5 $\mu\text{m}/\text{h}$ for a ZrO_2 sample and from 2.2 $\mu\text{m}/\text{h}$ to 5.2 $\mu\text{m}/\text{h}$ for an Si_3N_4 sample.

To ensure the same sputtering rate of 11.5 $\mu\text{m}/\text{h}$ at a small angle of incidence, the discharge current of $I_d = 2 \text{ A}$ should be increased to $\sim 5 \text{ A}$, and this results in overheating the accelerating grid and other parts of the experimental system. It means that an increase in the etching rate without increasing the beam power prevents the beam source from heating up to inadmissible temperature.

In addition, sputtering a ceramic sample with fast argon atoms at a large angle of incidence on its surface allows not only significantly increases the surface layer stripping rate but also ensures polishing of the surface to a high finishing class.

5. Conclusions

1. Etching ceramic products with fast argon atoms at a large angle of incidence on the product surface allows an appreciable increase in the etching rate.
2. The etching rate increases at permanent flux density and energy of the fast argon atoms due to an increase in the sputtering coefficient at a large angle of incidence.
3. The possibility to increase the etching rate without increasing the beam power prevents from heating the equipment up to inadmissible temperature.
4. Etching ceramic products with fast argon atoms at a large angle of incidence to the product surface is accompanied with the surface polishing.

Author Contributions: Conceptualization, A.S.M., M.A.V. and S.N.G.; methodology, A.S.M. and M.A.V.; software, E.S.M.; validation, A.S.M., M.A.V. and Y.A.M.; formal analysis, Y.A.M.; investigation, E.S.M. and Y.A.M.; resources, E.S.M. and Y.A.M.; data curation, M.A.V. and Y.A.M.; writing—original draft preparation, A.S.M. and M.A.V.; writing—review and editing, A.S.M. and S.N.G.; visualization, E.S.M.; supervision, A.S.M. and S.N.G.; project administration, M.A.V.; funding acquisition, S.N.G. All authors have read and agreed to the published version of the manuscript.

Funding: This research was funded by the Russian Science Foundation, grant no. 23-19-00517.

Institutional Review Board Statement: Not applicable.

Informed Consent Statement: Not applicable.

Data Availability Statement: The data presented in this study are available on request from the corresponding author.

Acknowledgments: The study was carried out with the equipment of the center of collective use of MSUT "STANKIN".

Conflicts of Interest: The authors declare no conflicts of interest.

References

1. Bonacchi, D.; Rizzi, G.; Bardi, U.; Scrivani, A. Chemical stripping of ceramic films of titanium aluminum nitride from hard metal substrates. *Surf. Coat. Technol.* **2003**, *165*, 35–39. [[CrossRef](#)]
2. Conde, A.; Cristobal, A.B.; Fuentes, G.; Tate, T.; De Damborenea, J. Surface analysis of electrochemically stripped CrN coatings. *Surf. Coat. Technol.* **2006**, *201*, 3588–3595. [[CrossRef](#)]
3. Sen, Y.; Ürgen, M.; Kazmanli, K.; Çakir, A.F. Stripping of CrN from CrN-coated high-speed steels. *Surf. Coat. Technol.* **1999**, *113*, 31–35. [[CrossRef](#)]

4. Grigoriev, S.N.; Volosova, M.A.; Lyakhovetsky, M.A.; Mitrofanov, A.P.; Kolosova, N.V.; Okunkova, A.A. Technological Principles of Complex Plasma-Beam Surface Treatment of Al₂O₃/TiC and SiAlON Ceramics. *J. Manuf. Mater. Process.* **2023**, *7*, 205. [[CrossRef](#)]
5. Tobola, D.; Czechowski, K.; Wrońska, I.; Łętocha, A.; Miller, T. The effect of the coating stripping process on regenerated tool cutting edges. *J. Achiev. Mater. Manuf. Eng.* **2013**, *61*, 294–301.
6. Dobrzański, L.A.; Zukowska, L.W. Gradient PVD coatings deposited on the sintered tool materials. *Arch. Mater. Sci. Eng.* **2011**, *48*, 103–111.
7. Pakuła, D.; Staszuk, M.; Dobrzański, L.A. Investigations of the structure and properties of PVD coatings deposited onto sintered tool materials. *Arch. Mater. Sci. Eng.* **2012**, *58*, 219–226.
8. Rebole, R.; Martinez, A.; Rodriguez, R.; Fuentes, G.G.; Spain, E.; Watson, N.; Avelar-Batista, J.C.; Housden, J. Microstructural and tribological investigations of CrN coated, wet-stripped and recoated functional substrates used for cutting and forming tools. *Thin Solid Films* **2004**, *469–470*, 466–471. [[CrossRef](#)]
9. Marimuthu, S.; Kamara, A.M.; Whitehead, D.; Mativenga, P.T.; Li, L. Laser removal of TiN coatings from WC micro-tools and in-process monitoring. *Opt. Laser Technol.* **2010**, *42*, 1233–1239. [[CrossRef](#)]
10. Schubert, E.; Schutte, K.; Emmel, A.; Bergmann, H.W.; Hans, W. Excimer laser assisted TiN and WC removal from tools as a novel decoating technology. *Proc. SPIE* **1995**, *2502*, 654–663. [[CrossRef](#)]
11. Primus, T.; Hlavinka, J.; Zeman, P.; Brajer, J.; Šorm, M.; Čermák, A.; Kožmín, P.; Holešovský, F. Investigation of Multiparameter Laser Stripping of AlTiN and DLC C Coatings. *Materials* **2021**, *14*, 951. [[CrossRef](#)]
12. Kaufman, H.R. Broad-beam ion sources. *Rev. Sci. Instrum.* **1990**, *61*, 230–235. [[CrossRef](#)]
13. Kaufman, H.R.; Hughes, W.E.; Robinson, R.S.; Tompson, G.R. Thirty-eight-centimeter ion source. *Nucl. Instrum. Meth. Phys. Res. B* **1989**, *37–38*, 98–102. [[CrossRef](#)]
14. Hayes, A.V.; Kanarov, V.; Vidinsky, B. Fifty-centimeter ion beam source. *Rev. Sci. Instrum.* **1996**, *67*, 1638–1641. [[CrossRef](#)]
15. Oks, E.M.; Vizir, A.V.; Yushkov, G.Y. Low-pressure hollow-cathode glow discharge plasma for broad beam gaseous ion source. *Rev. Sci. Instrum.* **1998**, *69*, 853–855. [[CrossRef](#)]
16. Vizir, A.V.; Yushkov, G.Y.; Oks, E.M. Further development of a gaseous ion source based on low-pressure hollow cathode glow. *Rev. Sci. Instrum.* **2000**, *71*, 728–730. [[CrossRef](#)]
17. Engelko, V.; Yatsenko, B.; Mueller, G.; Bluhm, H. Pulsed electron beam facility (GESA) for surface treatment of materials. *Vacuum* **2001**, *62*, 211–216. [[CrossRef](#)]
18. Metel, A.S. Compression of pulsed electron beams for material tests. *Mech. Ind.* **2017**, *18*, 708. [[CrossRef](#)]
19. McDaniel, E.W. *Collision Phenomena in Ionized Gases*; Wiley: New York, NY, USA, 1964; 775p.
20. Kaminsky, M. *Atomic and Ionic Impact Phenomena on Metal Surfaces*; Springer: Berlin/Heidelberg, Germany, 1965; 402p.
21. Metel, A.S.; Grigoriev, S.N.; Volosova, M.A.; Melnik, Y.A.; Mustafaev, E.S. Compression of a beam of fast argon atoms for surface polishing. *Instrum. Exp. Tech.* **2022**, *65*, 910–917. [[CrossRef](#)]
22. Phelps, A.V. Cross sections and swarm coefficients for nitrogen ions and neutrals in N₂ and argon ions and neutrals in Ar for energies from 0.1 eV to 10 keV. *J. Phys. Chem. Ref. Data* **1991**, *20*, 557–573. [[CrossRef](#)]
23. Phelps, A.V.; Greene, C.H.; Burke, J.P. Collision cross sections for argon atoms with argon atoms for energies from 0.01 eV to 10 keV. *J. Phys. B At. Mol. Opt. Phys.* **2000**, *33*, 2965–2981. [[CrossRef](#)]
24. Eckstein, W. Sputtering Yields. In *Sputtering by Particle Bombardment*; Topics in Applied Physics; Springer: Berlin/Heidelberg, Germany, 2007; Volume 110, pp. 33–187. [[CrossRef](#)]

Disclaimer/Publisher’s Note: The statements, opinions and data contained in all publications are solely those of the individual author(s) and contributor(s) and not of MDPI and/or the editor(s). MDPI and/or the editor(s) disclaim responsibility for any injury to people or property resulting from any ideas, methods, instructions or products referred to in the content.